scientific reports

Check for updates

OPEN

Design and bioactivity evaluation of a novel autotaxin inhibitor with anti-hepatic fibrosis effects

Yuzheng Liu[1,5], Dan Luo[2,5], Hongwen Leng[1,5], Chaolun Gu[1], Qingrong Ding[1], Lin Zhao[1], Xinxin Chao[3], Hanxia Wang[3], Yueteng He[3], Silu Zhu[2], Guanhua Ai[1]✉ & Weijie Peng[1,3,4]✉

Autotaxin (ATX) is considered as a serum marker of hepatic fibrosis, which is positively correlated with the degree of hepatic fibrosis. However, there are no clinical studies on anti-hepatic fibrosis drugs targeting ATX. This study attempts to find novel ATX small molecule inhibitors based on virtual screening methods including two-dimensional similarity search, pharmacophore screening, molecular docking, drug-like properties and ADMET filtration, combined with biological evaluation. An ATX inhibitor (IC50 = 43.05 μmol/L) is discovered by our screening strategy. In vivo result show that the novel ATX inhibitor represents excellent anti-hepatic fibrosis effects in mice. This screening strategy had potential significance for the discovery of ATX inhibitors in the future.

Liver fibrosis is a major health problem and is caused by a series of reasons such as alcohol, drugs, cholestasis. Aim of the therapeutic efforts is to reduce the progression of liver fibrosis and thus prevent further deterioration of the disease. With the novel technology and potential pathogenesis of liver fibrosis are continuously expanding. Unfortunately, there are currently no effective drugs for the treatment of liver fibrosis.

Autotaxin (ATX), an extracellular enzyme, has lysophospholipase D activity. ATX can cleave the primary substrate lysophosphatidylcholine (LPC) to lysophosphatidic acid (LPA)[1]. LPA exerts its biological actions by the activation of six G-protein coupled receptors (GPCRs). To date, these GPCRs are involved in LPA signalling (including LPA 1–6 receptors). LPA signaling through its six receptors lead to the induction of several downstream signaling pathways that cause a variety of biological effects such as cell proliferation, migration, angiogenesis, et al.. Clinical case reports find that ATX in serum is positively correlated with the degree of liver fibrosis. Clinical studies also find that patients with viral infections (HBV and HCV) has higher ATX levels in serum. They have a higher incidence of cirrhosis and hepatocellular carcinoma. Preliminary studies have shown that LPA can activate hepatic stellate cells and promote collagen secretion. Therefore, ATX is also considered to be an effective serum marker of hepatic fibrosis and a target for the development of anti-hepatic fibrosis drugs[2].

Several early ATX inhibitors are derived from LPA analogues or other biologically active lipids. The first patent for ATX inhibitors is based on lipid analogues for cancer treatment. A series of imidazole derivatives develop by Merck have shown a certain inhibitory effect on ATX. The IC50 is between 1 and 10 μmol/L. Over the past year, some new ATX inhibitors had achieved exciting results. The non-carboxylic ATX inhibitors were reported to reduce melanoma metastasis and chemosensitivity of breast cancer stem cells. Galapagos et al.. reported GLPG1690 reduced extracellular matrix deposition in mice with bleomycin-induced pulmonary fibrosis[3], and GLPG1690 was already in phase 3 trial for idiopathic pulmonary fibrosis[4]. Jun Se Kim et al. reported a Novel Autotaxin Inhibitor, BBT-877, which is a novel ATX inhibitor used in clinical treatment of idiopathic pulmonary fibrosis. However, the effects of BBT-877 on drug resistance and metastasis in ovarian CSCs remain unknown. In this study, they aimed to investigate the effects of BBT-877 on drug resistance and intraperitoneal metastasis of EOC[5]. Jacopo Simonetti et al. reported Phase III clinical efficacy of an autotraxin inhibitor, Ziritaxentat. Combining autotaxin inhibitors with existing anti-fibrotic agents is considered for enhanced therapeutic effects. Large phase III trials assessed Ziritaxestat but yielded disappointing results, highlighting the importance of long-term observation and clinical outcomes in clinical research[6].

These ATX inhibitors above are mainly used in the treatment of tumors, pulmonary fibrosis, melanoma and so on. Although ATX plays an important role in the formation of liver fibrosis, so far, no clinical small

[1]Jiangxi Academy of Medical Sciences, and Hospital of Nanchang University, Bayi Road 461, Nanchang 330006, Jiangxi, People's Republic of China. [2]School of Basic Medicine, Medical College, Nanchang University, Bayi Road 461, Nanchang 330006, Jiangxi, People's Republic of China. [3]School of Pharmaceutics, Medical College, Nanchang University, Bayi Road 461, Nanchang 330006, Jiangxi, People's Republic of China. [4]School of Pharmaceutics, Gannan Medical University, Ganzhou 341000, Jiangxi, People's Republic of China. [5]Yuzheng Liu, Dan Luo and Hongwen Leng contributed equally to this work. ✉email: ai_guanhua@126.com; Pengweijie@gmu.cn

molecule drugs been reported for the treatment of liver fibrosis. In order to try to solve this problem, we focus on the combination of rational drug design[7–9], drug-like filtration[10,11], ADMET pre-prediction methods[12] and biological methods to study the small molecule ATX inhibitors. The entire protocol would be helpful for discovery of new ATX inhibitors.

Materials and methods

Protein and ligand preparation

The nine ATX crystal complexes (PDB ID: 3WAX, 4ZG7, 5KXA, 5LIA, 5L0E, 5LQQ, 5M7M, 5M0D and 5OHI, respectively) were downloaded directly from PDB database without any processing. The specs database was obtained from a commercial company (Shanghai Taozhu Biotechnology Co., Ltd., China) with a two-dimensional structure without any processing.

Find similar molecules by fingerprints

Nine ligand compounds from protein data bank (PDB ID: 3WAX, 4ZG7, 5KXA, 5LIA, 5L0E, 5LQQ, 5M7M, 5M0D and 5OHI, respectively) were selected as query molecules to extract similar molecules from Zinc-Specs Database. To find similar molecules by fingerprint, the Find Similar Molecules by Fingerprints protocols by Discovery Studio (DS) software were used in this study. The three similarity measures were applied from the protocols, namely, Tanimoto[13,14]: SA/(SA + SB + SC), Cosine[15]: SA/[(SA + SB)×(SA + SC)]$^{0.5}$ and Target[16]: SA/(SA + SC), where SA, SB, and SC are defined as: SA indicate the number of AND bits, SB indicate the number of bits in the target but not the reference, SC indicate the number of bits in the reference but not the target. In each measure, two fingerprints were used: ECFC_4[17]and ECFP_4[18–20].

Generation and validation of the pharmacophore model

The receptor-ligand pharmacophore generation protocol by DS software was used to create a pharmacophore model. The generation of pharmacophores involves the following processes. First, a set of features (including hydrogen bond acceptor, hydrogen bond donor, hydrophobic, negative ionizable, positive ionizable and ring aromatic) from the binding ligand are identified. Second, the pharmacophore models are ranked based on its sensitivity and specificity, the top models are returned. Then this pharmacophore models are enumerated and its selectivity is estimated based on a Genetic Function Approximation (GFA) model[21]. In this step, we used the parameters including: Minimum Features option was set as 3, Maximum Features was defined as 7, and the remaining parameters were retained as default values.

To perform the pharmacophore validation, the validation option of the Receptor-Ligand Pharmacophore Generation protocol by DS software was set to true. The aim of pharmacophore validation was to assess the quality of pharmacophore models. An important property of a reliable pharmacophore model was able to accurately distinguish active and inactive compounds from the test set. A data set containing inactive and active compounds were required to perform the pharmacophore validation. Nine compounds with known ATX inhibitory activity were selected as the active compounds from PDB database. These compounds were also used as query molecules during finding similar molecules by fingerprints. 450 inactive compounds were randomly selected from Maybrige database. These compounds share similar molecular sizes with active compounds.

Pharmacophore screening

In order to carry out the pharmacophore screening, the Screen Library protocol by DS software was used in this process. The principles of the pharmacophore screening were firstly analyzed large collections of pharmacophore features, then comparing a set of ligands to the most relevant pharmacophore models. To choose lead compounds, the resulting molecules from the find similar molecules by fingerprints step were mapped to the best pharmacophore model. In this step, the minimum features parameter was set as 3, maximum features was set as 5, and the remaining parameters were retained as default values.

Molecular docking

For completing molecular docking, the LibDock program of DS software were selected to perform this task. LibDock is a high-throughput docking algorithm for docking ligands to the active site of a specific receptor. Ligand conformations are aligned to hot spots and the best ranking poses are saved. The specific implementation process is as follows in this study. Firstly, a CHARMm force field was used to add the force field to the ATX receptor. Then the binding site sphere was defined from selecting the fifth PDB site of ATX. Finally, the docking poses were ranked by the docking score.

Lipinski and Veber rules, and ADMET analysis

Lipinski and Veber Rules protocol of DS software was used to further filter the compounds which were obtained after the above molecular docking. Where default parameters were left. The good bioavailability is critical for oral drugs to exert their drug effects in vivo. The well known "Rule of Five" research was pioneered by Lipinski et al. for selecting drug-like molecules in 1997. The research suggested that a drug-like molecule share the following properties: ≤5 hydrogen bond donors, ≤10 hydrogen bond acceptors, molecular weight ≤ 500, LogP ≤ 5[22]. ADMET was also known as the Absorption, Distribution, Metabolism, Excretion, and Toxicity properties of a molecule in vivo[23–28]. During the early drug discovery, optimizing these properties were crucial for the drug development process. Using the ADMET descriptors were able to avoid expensive reformulation later by eliminating compounds with unfavorable ADMET features early. Application of ADMET descriptors was also evaluated the proposed structural refinements and further improved the compounds of ADMET characteristics prior to the synthesis. The ADMET protocol of DS software was used in this step. All parameters were retained as default values.

Enzyme-based ATX activity assay

The assay was exerted with reference to previous literature[29]. Briefly, the inhibitors were tested using the Amplex® Red Phospholipase D Assay Kit (A12219). A total volume of 200 μL was used in per microplate well. A volume of 100 μL samples solution containing ATX (4nM) and different concentrations of inhibitors was used for each reaction. A working solution of 100 μM Amplex Red reagent containing 2 U/mL horseradish peroxidase (HRP), 0.2 U/mL choline oxidase and 0.5 mM LPC (16:0) were prepared. The reactions were begun by adding 100 μL of the Amplex Red reagent/HRP/choline oxidase/lecithin working solution to each microplate well containing the above 100 μL of samples solution. Incubate the reactions for one hour at 37 °C, protected from light. The fluorescence was measured in a fluorescence microplate reader using excitation at 530 ± 12.5 nm and emission detection at 590 ± 17.5 nm. The assay were used the mean values obtained from two independent experiments. The IC_{50} values were obtained using the GraphPad Prism 5 software. The reported ATX inhibitor (compound 4) was > 95% pure by LC-MS analysis (Fig. S1 and Fig. S2). Compound 4 was purchased from specs through TopScience Co., Ltd for in vitro experiments. Compound 4 was synthesized by mjinbiotech company for in vivo experiments.

Mice models of liver fibrosis treated with ATX inhibitor

The male mice were obtained from Laboratory Animal Unit. The study protocol was approved by the Institutional Ethics Committee of Jiangxi Academy of Medical Science (grant no.: JXAMS-EWC-2021012). This study was conducted in strict accordance with the recommendations of the guide for the care and use of laboratory animals issued by the Ministry of science and technology of China. The study is reported in accordance with ARRIVE guidelines. Liver fibrosis was induced by intraperitoneal injection of CCl4 (20% CCl4 in rapeseed oil, 0.5 ml/100 g body weight, twice weekly) for 33 days. The mice were randomly divided into four groups: Group 1, normal control group with free access to food and water; Group 2, CCl4 alone; Group 3, CCl4 + inhibitor (7.5 mg/kg); Group 4, CCl4 + inhibitor (15 mg/kg); Group 5, CCl4 + inhibitor (30 mg/kg); Group 6, inhibitor (30 mg/kg) alone. The inhibitor was administered by intraperitoneal injection (once a day, six times a week), starting from the 14th day of the CCl_4 injection for a total of 20 days.

Preparation of blood sample and tissue homogenate

Then the blood samples was collected from mice orbit and allowed to clot at room temperature for 60 min. The samples were centrifuged (3000r/min, 10 min) to recover the serum from each supernatant and stored at 20℃. After the blood collection, the liver of mice was removed. Live samples were fixed in 4% polyformaldehyde and embedded in paraffin. The embedded samples was cut as 4 μm sections, then processed routinely for Sirius red staining.

The measures of liver function, blood glucose and blood lipid, and renal function

The serum alanine aminotransferase (ALT), aspartate aminotransferase (AST), ALT/AST, glutamyl transpeptidase (GT), alkaline phosphatase (ALP), blood glucose and blood lipid, and renal function were each assayed using kits from Mindray (China). The ALT and AST were measured the pyruvate and oxaloacetate, respectively, which were produced from 2,4-dinitrophenylhydrazine.

Statistical treatment

Data were shown as mean ± S.D. Graph pad prism 5.0 was used for statistical analysis. After confirming that the data were normally distributed and exhibited equivalent variances, mean values among groups were compared by Student's two-tailed t test or two-way ANOVA with Tukey's test. A p value < 0.05 was considered significant for statistical comparisons.

Results and discussion

In order to obtain the novel ATX inhibitors, the overall process of this design was shown in the Fig. 1.

Finding similar molecules by fingerprints

In this study, we used the find similar molecules by fingerprints protocol to screen a specs database based on nine reported active inhibitors of ATX as shown in Table 1. The principle of finding similar molecules was based on the concept of structurally similar molecules are likely to have similar bioactivity. Each running generated 500 most similar molecules to the nine reference molecules using three measures (Tanimoto, Cosine, Target) and every measure used two fingerprint (ECFC_4 and ECFP_4). The use of three measures and two fingerprints would increase the confidence levels from the screening results. As the results, each molecule screening would produce the most 3000 molecules. As nine molecules were used as queried molecules, 27,000 similar molecules were returned from the screening.

Generation and validation of pharmacophore modeling

The crystallography structure of ATX enzyme (PDB ID: 5KXA) was used to create pharmacophore modeling using the receptor-ligand pharmacophore generation protocol. At the same time, a test set consisting of 9 active (Table 1) and 450 inactive molecules (supporting document: Molecule.sd) was used to verify the quality of pharmacophore model. A total of 20 pharmacophore models were produced by using this protocol. From the validation results of 20 pharmacophore model against the test set (Table 2), the first pharmacophore (Pharmacophore_01) was exhibited the best selectivity (0.88889) and specificity (0.42000). The Pharmacophore_01 was also obtained a high predictive accuracy from the ROC curve (Fig. 2). The 20 pharmacophores summary was shown in Table 3. The selective score was shown as positive number from the first to eleventh pharmacophore models. The other pharmacophore models were obtained the selective scores as negative number. A higher selectivity score was

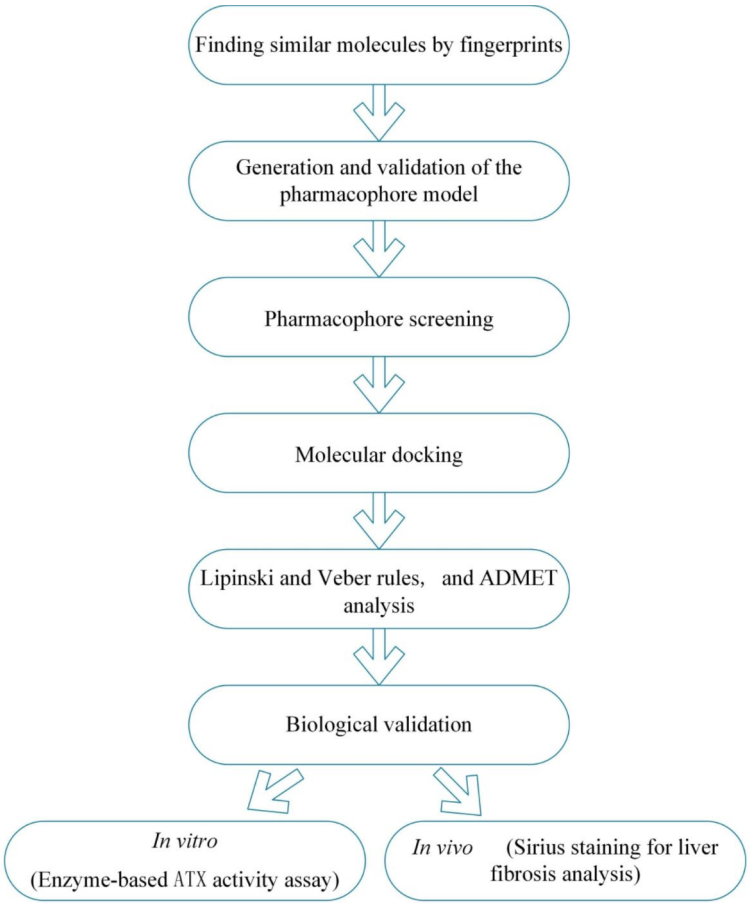

Fig. 1. The overall flow chart of this study.

indicated more excellent selectivity for a pharmacophore model. The feature set from the table was listed the pharmacophore features of each pharmacophore model, such as hydrogen bond acceptor (A), hydrogen donor (D), hydrophobic (H), and ring aromatic (R), etc. According to the analyses above, the Pharmacophore_01 has the best discriminatory ability against test set compounds. Pharmacophore_01 was shown in Fig. 3, which included five pharmacophore features and some excluded volumes, namely, three hydrophobic features, one ring aromatic and one negative ionizable feature.

Pharmacophore screening

The purpose of pharmacophore screening was to further narrow down the molecules. We used the Pharmacophore_01 to screen the 27,000 molecules which were obtained from the find similar molecules by fingerprints. Finally, a total of 4073 molecules with Fit values greater than 2.0 were selected to further filter by subsequent molecular docking.

Molecular docking, Lipinski and Veber rules, and ADMET analysis

Molecular docking was used to identify the interactions between ligand & receptor/enzyme, and searching the best orientation of ligand to a specific enzyme/receptor. In our study, the 4073 molecules received by the Pharmacophore_01 model and were further docked into the active cite of ATX (PDB ID: 5KXA) by using the LibDock algorithm of DS. To complete the docking, the active sites were defined as a red sphere (Fig. 4). Finally, the top ranked 1000 molecules according to LibDock score were selected to further filter by Lipinski and Veber rules. Lipinski and Veber proposed that molecular characteristics affect oral bioavailability of candidate drugs. The candidate drugs with good oral bioavailability are generally considered to possess the following characteristics: LogP ≤ 5, molecular weight ≤ 500, ≤ 5 hydrogen bond donors, ≤ 10 hydrogen bond acceptors. As a result, 244 molecules were successfully received using this method. Then the 244 molecules were further filtered by ADMET. ADMET descriptors of ligands was to calculate the Absorption (A), Distribution (D), Metabolism (M), Excretion (E), and Toxicity (T) properties. All of 244 molecules were successfully passed the filtration. Finally, several compounds based on the screening results above were selected for biological validation.

Category	Number	Structure
Active compounds	Active 1	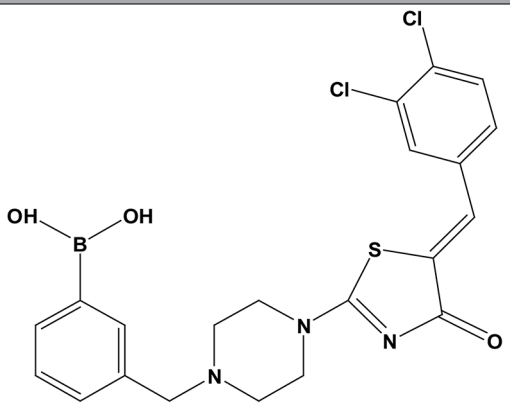
	Active 2	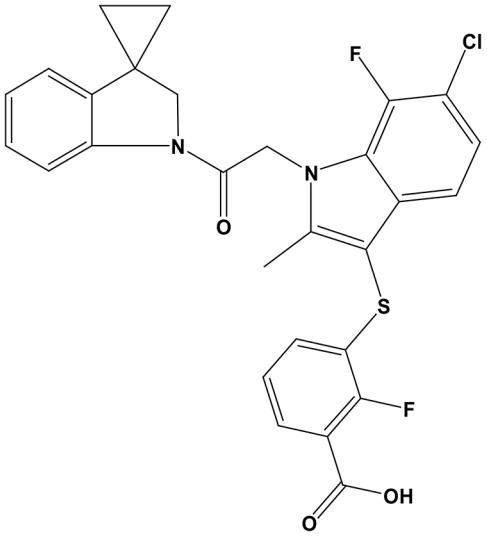
	Active 3	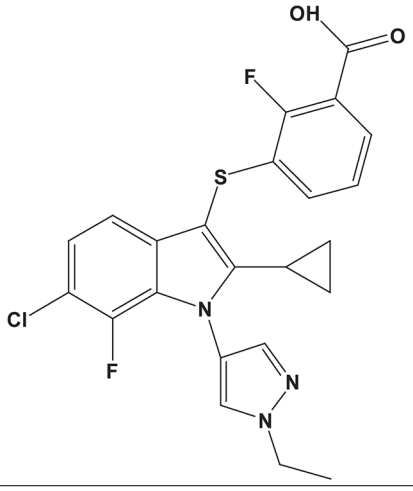
Continued		

Category	Number	Structure
	Active 4	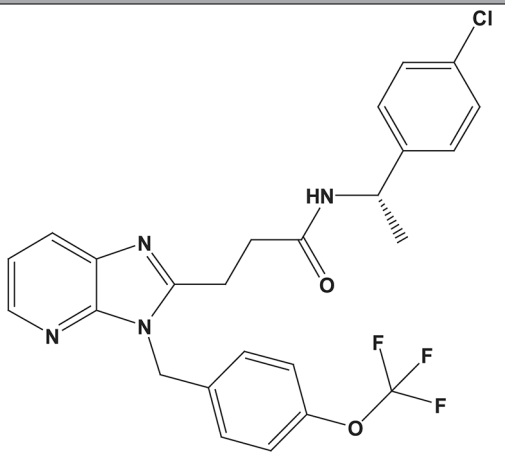
	Active 5	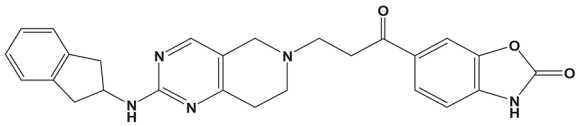
	Active 6	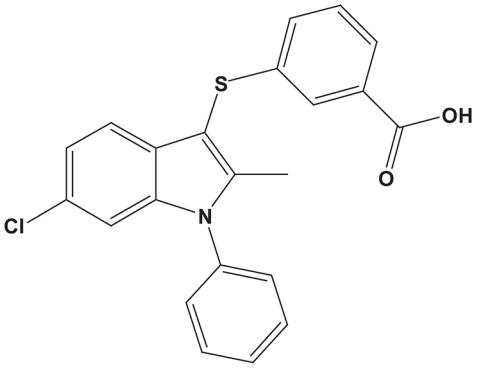
	Active 7	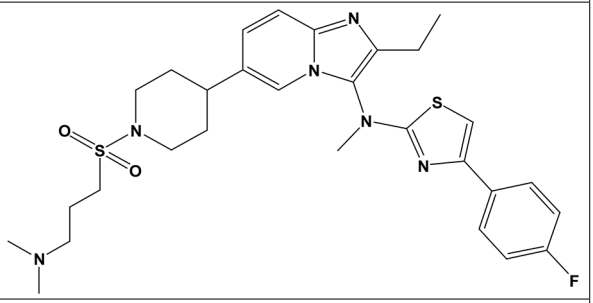

Continued

Category	Number	Structure
	Active 8	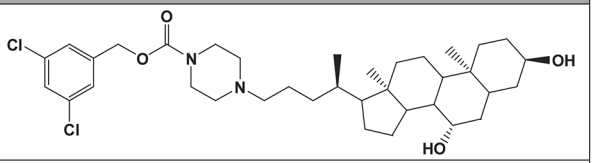
	Active 9	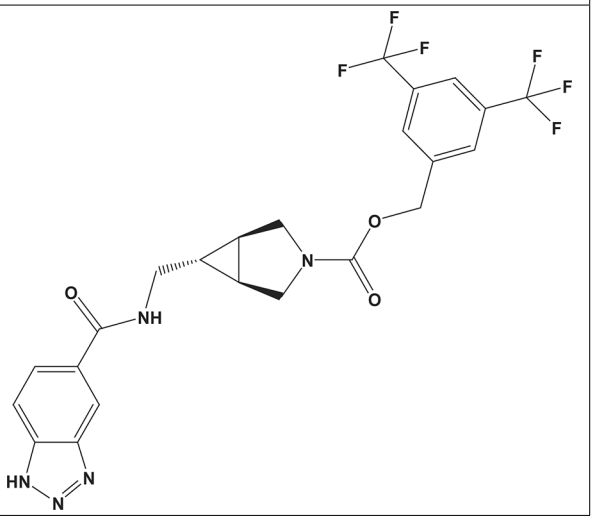

Table 1. The active molecules of ATX.

Pharmacophore	Total actives	Total inactives	True positives	True negatives	False positives	False negatives	Sensitivity	Specificity
Pharma-cophore-01	9	450	8	189	261	1	0.88889	0.42000
Pharma-cophore-02	9	450	9	165	285	0	1	0.36667
Pharma-cophore-03	9	450	9	130	320	0	1	0.28889
Pharma-cophore-04	9	450	9	78	372	0	1	0.17333
Pharma-cophore-05	9	450	9	49	401	0	1	0.10889
Pharma-cophore-06	9	450	9	74	376	0	1	0.16444
Pharma-cophore-07	9	450	2	424	26	7	0.22222	0.94222
Pharma-cophore-08	9	450	2	434	16	7	0.22222	0.96444
Pharma-cophore-09	9	450	2	435	15	7	0.22222	0.96667
Pharma-cophore-10	9	450	9	30	420	0	1	0.066667
Pharma-cophore-11	9	450	9	35	415	0	1	0.077778
Pharma-cophore-12	9	450	9	66	384	0	1	0.14667
Pharma-cophore-13	9	450	9	55	395	0	1	0.12222
Pharma-cophore-14	9	450	2	82	368	7	0.22222	0.18222
Pharma-cophore-15	9	450	9	174	276	0	1	0.38667
Pharma-cophore-16	9	450	9	17	433	0	1	0.037778
Pharma-cophore-17	9	450	9	17	433	0	1	0.037778
Pharma-cophore-18	9	450	9	30	420	0	1	0.066667
Pharma-cophore-19	9	450	9	30	420	0	1	0.066667
Pharma-cophore-20	9	450	9	30	420	0	1	0.066667

Table 2. The validation results of pharmacophore model against test set.

Enzyme-based ATX activity assay

A small amount of compounds were selected through the above screening to evaluate the in vitro activity against ATX enzyme using the Amplex Red PLD assay kit. LPC (16:0) was used as substrate. Among them, compound 4 (Fig. 5) showed a good inhibition rate of ATX (IC_{50} = 43.05 μmol/L).

Interaction analysis

In order to further elucidate the action mode of compound 4 with ATX enzyme, the docking results showed compound 4 could interact well with ATX enzyme. As shown in Fig. 5, compound 4 occupied a wide cavity

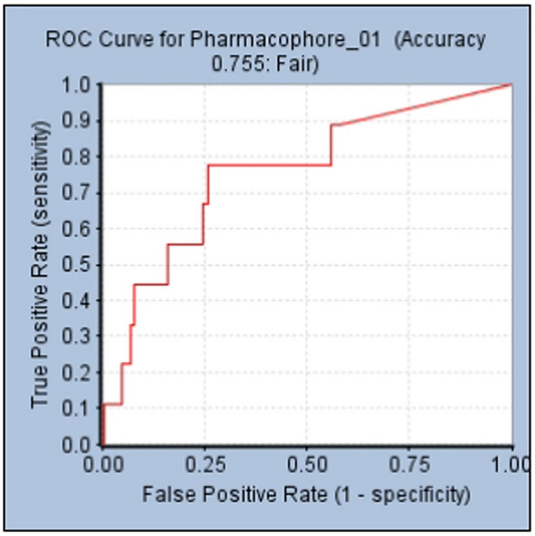

Fig. 2. The ROC curve for Pharmacophore_01.

Pharmacophore	Number of features	Feature set	Selectivity score
Pharmacophore_01	5	HHHNR	2.2999
Pharmacophore_02	4	HHHN	2.0482
Pharmacophore_03	4	HHNR	1.9582
Pharmacophore_04	4	HHNR	1.9582
Pharmacophore_05	3	HNR	1.8380
Pharmacophore_06	4	HHNR	1.3031
Pharmacophore_07	3	HHN	1.2728
Pharmacophore_08	3	HHN	1.2728
Pharmacophore_09	3	HHN	1.2728
Pharmacophore_10	3	HNR	1.1829
Pharmacophore_11	3	HNR	1.1829
Pharmacophore_12	4	HHHR	− 0.26794
Pharmacophore_13	4	AHHR	− 0.26794
Pharmacophore_14	3	AHH	− 0.29816
Pharmacophore_15	3	HHH	− 0.29816
Pharmacophore_16	3	AHR	− 0.38815
Pharmacophore_17	3	AHR	− 0.38815
Pharmacophore_18	3	HHR	− 0.38815
Pharmacophore_19	3	HHR	− 0.38815
Pharmacophore_20	3	HHR	− 1.0433

Table 3. Pharmacophore summary.

surrounded by a lot of amino acids. It was also observed that a benzene ring of compound 4 formed two π-π interactions with HIS (A:252) and TYR(A:215). The triazole group of compound 4 also formed one π-π interaction with TRP(A:255). Another benzene ring of compound 4 formed one sigma-π interaction with TRP(A:276). The action mode was revealed that these amino acids may played an important role in the enzymatic catalysis of ATX.

Compound 4 inhibits fibrosis and inflammation of liver in vivo

The normal control group had normal histological structures (Fig. 6A). Mice was treated with CCl4 alone revealed a marked increase in the extent of liver fibrosis (Fig. 6B). Compared with the CCl4 alone model group, pathological conditions of the liver in the compound 4 of middle-dose group (15 mg/kg) and the high-dose group (30 mg/kg) administration were significantly improved, and the proliferation of hepatic fibrous connective tissue was significantly reduced in the low-dose group, middle- and high-dose group (Fig. 6C–E). The compound 4 (30 mg/kg) showed stronger anti-liver fibrosis effects than compound 4 (15 mg/kg and 7.5 mg/kg). The gold standard of tissue sections showed that the compound 4 had a significant inhibitory effect on the formation of

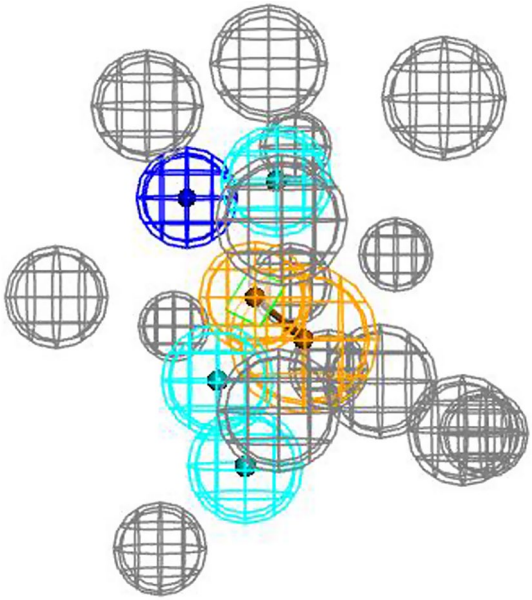

Fig. 3. The properties of top-ranked pharmacophore model (Pharmacophore_01). Pharmacophore is a model based on the characteristic elements of pharmacodynamics. The pharmacodynamic characteristic elements are mainly divided into seven types, including: hydrogen bond donors, hydrogen bond acceptors, positive and negative charge centers, aromatic ring centers, hydrophobic groups, hydrophilic groups, and geometric conformational volume collisions. Pharmacophore features are color-coded: pale blue, hydrophobic feature; orange yellow, ring aromatic feature; purple, negative ionizable feature.

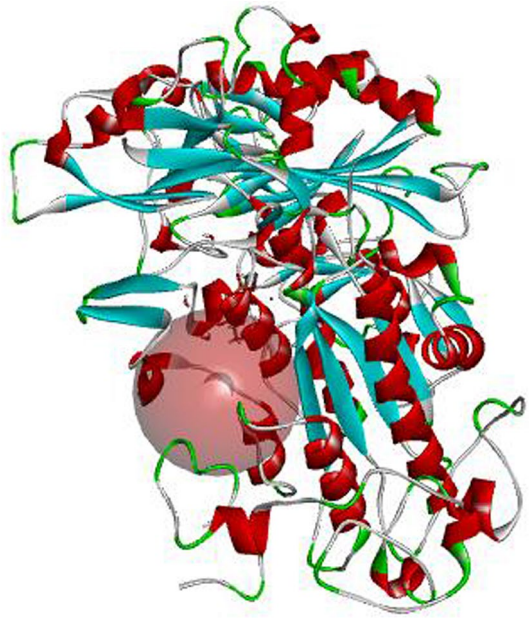

Fig. 4. The molecular docking diagram. The active sites are represented by red spheres. The rest part is ATX enzyme.

liver fibrosis in mice. Additionally, the normal mice with compound 4 alone was shown no influences on liver (Fig. 6F).

In order to determine the effect of compound 4 on hepatitis (Table 4), we tested serum ALT, AST,

ALT/AST, GT, and ALP levels. ALT and AST levels were significantly decreased following compound 4 treatment compared the CCl4 alone model group. The result suggested that compound 4 had a good protective effect on liver function. In addition, blood glucose, blood lipid and renal function tests showed that there was no abnormal change in the high-dose group (30 mg / kg) compared with the normal control group (Table 4).

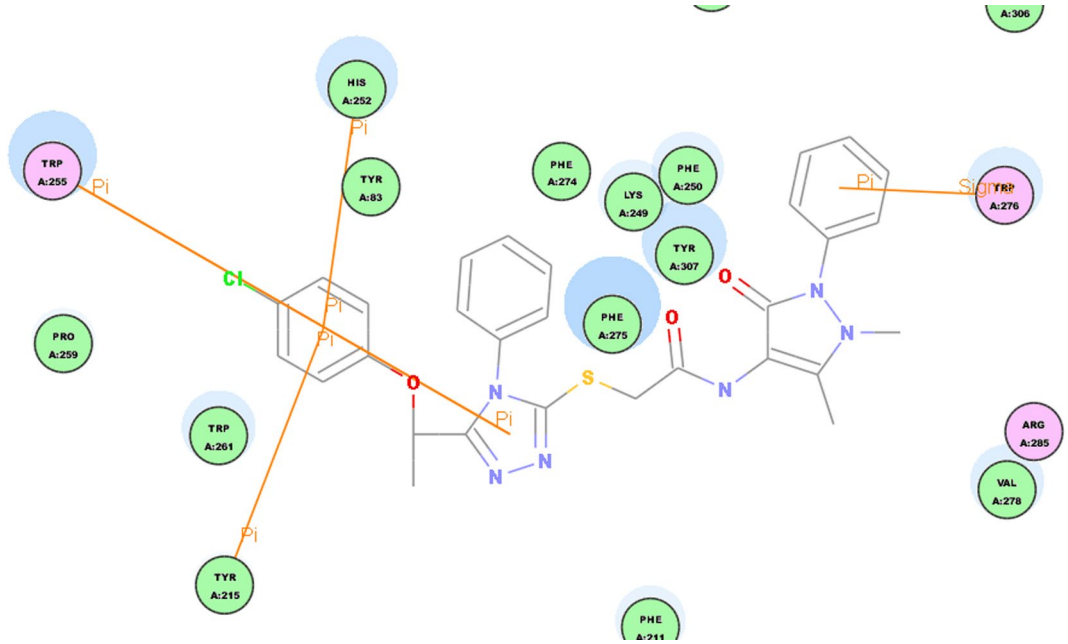

Fig. 5. Interactions between compound 4 with ATX enzyme. The compound 4 formed four π-π and one sigma-π interactions with ATX enzyme.

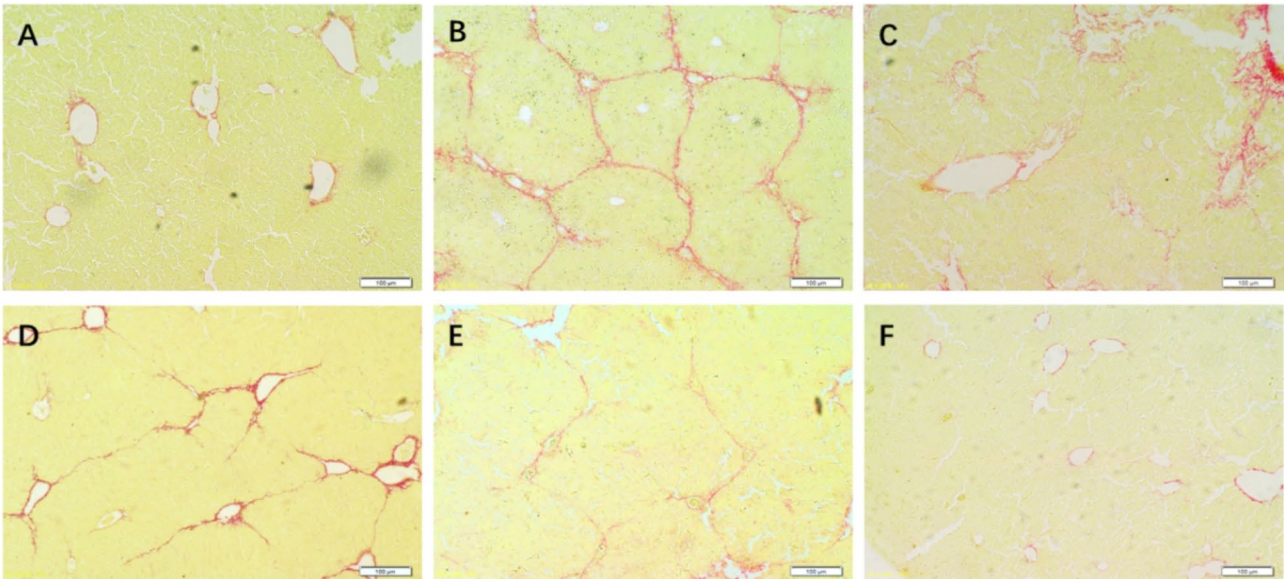

Fig. 6. Effects of the compound 4 on liver fibrosis in vivo. Liver sections stained with Sirius red. (**A**) The normal control group. (**B**) Model group. Mice were injected intraperitoneally with 20% CCl4 in rapeseed oil (0.5 ml/100 g body weight, twice weekly) for 33 days. (**C**–**E**) Model mice were intraperitoneally injected with the compound 4 of low-dose group (7.5 mg/kg), middle-dose (15 mg/kg), high-dose (30 mg/kg), respectively, starting from the 14th day of the CCl4 injection for a total of 20 days. (**F**) The normal mice treated with compound 4 of high-doze group (30 mg/kg) administration. Six random microscope fields were assessed. Magnification×10.

Since the pathological staining results and serological biochemistry indexes of compound 4 alone group were no difference when compared with control group, it was suggested that the compound 4 was safe for the treatment of liver fibrosis in mice. The present study aimed to design and screen effective compounds for suppressing liver fibrosis through standard models and indexes, however, the detailed mechanisms of ATX and its inhibitors involving liver fibrosis was unclear and would be the focus for the next stage.

Classify	Abbrevation	Full name	Unit	Normal control group	CCl_4 alone group	Inhibitor alone group	CCl_4+ inhibitor (15 mg/kg) group	CCl_4+ inhibitor (30 mg/kg) group
Liver functon	ALT	Number		8	6	9	7	6
		Alanine aminotransferase	U/L	65.4 ± 20.65	5634.42 ± 3967.36a	53.13 ± 10.43	1485.61 ± 791.10b	2548.75 ± 1485.87
	AST	Aspartate aminotransferase	U/L	175.78 ± 52.29	3683.75 ± 2613.96a	144.80 ± 39.95	1411.71 ± 1075.25b	2885.05 ± 2162.49
	GT	Glutamyl transpeptidase	U/L	3.93 ± 0.46	2.12 ± 2.05	2.38 ± 0.53	3.82 ± 2.14	4.80 ± 1.49
	ALP	Alkaline phosphatase	U/L	173.45 ± 43.91	137.67 ± 58.74	110.8 ± 35.36	73.86 ± 21.17	107.40 ± 36.39
Blood glucose and lipids	GLU	Glucose	mmol/L	4.77 ± 1.25	3.78 ± 2.00	5.20 ± 1.49	4.6 ± 1.25	4.29 ± 2.69
	TC	Total cholesterol	mmol/L	1.93 ± 0.63	2.39 ± 0.93	3.00 ± 0.04	1.44 ± 0.52	1.54 ± 1.02
	TG	Triglyceride	mmol/L	1.22 ± 0.47	0.95 ± 0.37	1.86 ± 0.30	1.01 ± 0.35	0.70 ± 0.35
	HDL	High density lipoprotein	mmol/L	1.63 ± 0.49	1.74 ± 0.84	2.18 ± 0.05	0.95 ± 0.33	1.14 ± 0.88
	LDL	Low density lipoprotein	mmol/L	0.15 ± 0.10	0.17 ± 0.15	0.44 ± 0.05	0.13 ± 0.10	0.10 ± 0.11
Renal function	UREA	Urea	mmol/L	6.03 ± 1.12	8.49 ± 4.06	4.51 ± 0.55	4.53 ± 1.00	9.24 ± 2.76
	CRE	Creatinine	Umol/L	11.45 ± 1.34	9.95 ± 5.15	6.38 ± 1.95	6.89 ± 3.46	11.00 ± 8.01
	URIC	Uric acid	Umol/L	141.58 ± 41.26	59.50 ± 79.95	125.10 ± 19.62	30.14 ± 20.38	63.50 ± 77.63

Table 4. Compound 4 inhibits inflammation of liver and effects on blood glucose, blood lipid and renal function in vivo. a. $P < 0.05$ vs. Control group; b. $p < 0.05$ vs. CCl4 group

Conclusion

The aim of the current work is to find novel ATX inhibitors. Our study combines a series of computer-aided drug design methods with in vitro and in vivo biological evaluation strategy. The application of the computer-aided drug design methods including molecule fingerprints, pharmacophore modeling and molecular docking, et al. The selected molecule by using computer-aided drug design methods are further verified by enzyme-based ATX activity assay and liver fibrosis evaluation in vivo. The study found compound 4 show significant inhibitory effects with IC50 values (43.05 μmol/L) against ATX enzyme. Compared with the CCl4 alone model group, the pathological condition of liver tissue in mice treat with compound 4 is significantly improved, and the proliferation of hepatic fibrous connective tissue are also significantly reduced. The resulting pharmacophore model and the entire screening strategy would help to discovery of new ATX inhibitors.

Data availability

The datasets used and/or analysed during the current study available from the corresponding author on reasonable request.

Received: 6 September 2024; Accepted: 21 March 2025
Published online: 01 April 2025

References

1. Sevastou, I. et al. Lysoglycerophospholipids in chronic inflammatory disorders: The PLA(2)/LPC and ATX/LPA axes. *Biochim. Biophys. Acta***1831**(1), 42–60 (2013).
2. Kaffe, E. et al. Hepatocyte autotaxin expression promotes liver fibrosis and cancer. *Hepatology* **65**(4), 1369–1383 (2017).
3. Nikolaou, A. et al. Autotaxin inhibitors: A patent review (2012–2016). *Expert Opin. Ther. Pat.* **27**(7), 815–829 (2017).
4. Maher, T. M. et al. Safety, tolerability, pharmacokinetics, and pharmacodynamics of GLPG1690, a novel autotaxin inhibitor, to treat idiopathic pulmonary fibrosis (FLORA): A phase 2a randomised placebo-controlled trial. *Lancet Respir. Med.* **6** (8), 627–635 (2018).
5. Kim, J. S. et al. BBT-877, a novel autotaxin inhibitor, abrogates drug resistance in epithelial ovarian cancer stem cells. *Anticancer Res.* **44**(3), 1131–1142 (2024).
6. Simonetti, J. et al. Experimental autotaxin inhibitors for the treatment of idiopathic pulmonary fibrosis. *Expert Opin. Investig. Drugs* **33**(2), 133–143 (2024).
7. Loganathan, L. et al. Computational and pharmacogenomics insights on hypertension treatment: Rational drug design and optimization strategies. *Curr. Drug Targets* (2019).
8. Wang, C. et al. Rational design of hybrid peptides: A novel drug design approach. *Curr. Med. Sci.* **39**(3), 349–355 (2019).
9. Kim, E. & Kim, C. Rational drug design approach of receptor tyrosine kinase type III inhibitors. *Curr. Med. Chem.* (2018).
10. Pal, S. et al. Ligand-based pharmacophore modeling, virtual screening and molecular docking studies for discovery of potential topoisomerase I inhibitors. *Comput. Struct. Biotechnol. J.* **17**, 291–310 (2019).
11. Mostashari-Rad, T., Saghaei, L. & Fassihi, A. Gp41 inhibitory activity prediction of theaflavin derivatives using ligand/structure-based virtual screening approaches. *Comput. Biol. Chem.* **79**, 119–126 (2019).
12. !!! INVALID CITATION !!!.
13. Baldi, P. & Hirschberg, D. S. An intersection inequality sharper than the Tanimoto triangle inequality for efficiently searching large databases. *J. Chem. Inf. Model.* **49**(8), 1866–1870 (2009).
14. Godden, J. W., Xue, L. & Bajorath, J. Combinatorial preferences affect molecular similarity/diversity calculations using binary fingerprints and Tanimoto coefficients. *J. Chem. Inf. Comput. Sci.* **40**(1), 163–166 (2000).
15. Yang, J. et al. EKF-GPR-Based fingerprint renovation for subset-based indoor localization with adjusted cosine similarity. Sensor (Basel) **18**(1) (2018).
16. Dror, I. E. et al. Cognitive issues in fingerprint analysis: inter- and intra-expert consistency and the effect of a 'target' comparison. *Forensic Sci. Int.* **208**(1–3), 10–17 (2011).

17. Arif, S. M., Holliday, J. D. & Willett, P. Analysis and use of fragment-occurrence data in similarity-based virtual screening. *J. Comput. Aided Mol. Des.* **23**(9), 655–668 (2009).
18. Pasupa, K. & Kudisthalert, W. Virtual screening by a new Clustering-based weighted similarity extreme learning machine approach. *PLoS One* **13**(4), e0195478 (2018).
19. Zhang, Y. et al. An integrated virtual screening approach for VEGFR-2 inhibitors. *J. Chem. Inf. Model.* **53**(12), 3163–3177 (2013).
20. Wang, Z. et al. P-glycoprotein substrate models using support vector machines based on a comprehensive data set. *J. Chem. Inf. Model.* **51**(6), 1447–1456 (2011).
21. Sivakumar, P. M., Geetha Babu, S. K. & Mukesh, D. QSAR studies on chalcones and flavonoids as anti-tuberculosis agents using genetic function approximation (GFA) method. *Chem. Pharm. Bull. (Tokyo)* **55**(1), 44–49 (2007).
22. Lipinski, C. A. Chris Lipinski discusses life and chemistry after the rule of five. *Drug Discov Today* **8**(1), 12–16 (2003).
23. Wu, Z. et al. ADMET evaluation in drug discovery. 19. Reliable prediction of human cytochrome P450 inhibition using artificial intelligence approaches. *J. Chem. Inf. Model.* (2019).
24. Bansode, P. et al. Evaluation of drug candidature: in Silico ADMET, binding interactions with CDK7 and normal cell line studies of potentially anti-breast cancer enamidines. *Comput. Biol. Chem.* **83**, 107124 (2019).
25. Kalirajan, R. et al. In-silico design, ADMET screening, MM-GBSA binding free energy of some novel isoxazole substituted 9-anilinoacridines as HER2 inhibitors targeting breast cancer. *Curr. Drug Res. Rev.*, (2019).
26. Kataria, R. & Khatkar, A. In-silico design, synthesis, ADMET studies and biological evaluation of novel derivatives of chlorogenic acid against urease protein and *H. Pylori* bacterium. *BMC Chem.* **13**(1), 41 (2019).
27. Sahu, S. et al. In silico ADMET study, docking, synthesis and antimalarial evaluation of thiazole-1,3,5-triazine derivatives as Pf-DHFR inhibitor. *Pharmacol. Rep.* **71**(5), 762–767 (2019).
28. El-Helby, A. A. et al. Design, synthesis, in silico ADMET profile and GABA-A Docking of novel phthalazines as potent anticonvulsants. *Arch. Pharm. (Weinheim)* **352**(5), e1800387 (2019).
29. Nikolaou, A. et al. Hydroxamic acids constitute a novel class of autotaxin inhibitors that exhibit in vivo efficacy in a pulmonary fibrosis model. *J. Med. Chem.* **61**(8), 3697–3711 (2018).

Acknowledgements

The work was supported by National Nature Science Foundation of China (Grant No: 81860327 and 82160677), The 5511 Talent Planning of Jiangxi Province (20165BCB18002), Key Innovation Project of Jiangxi Province (20171ACG70007), Science and Technology Plan of Jiangxi Provincial Health and Family Planning Commission (20175521) and Science and Technology Research Project of Jiangxi Provincial Department of Education (GJJ150061), Academic and technical Leaders Program in Jiangxi Province (GrantNo. 20204BCJL22052).

Author contributions

W.P. and G.A. designed the study and wrote the manuscript, Y.L., D.L. and H.L. performed the biological verification. C.G., Q.D., L.Z., X.C., H.W, Y.H. and S.Z. participate in biological validation, G.A. completed the computer-aided drug design work.

Declarations

Competing interests

The authors declare no competing interests.

Additional information

Supplementary Information The online version contains supplementary material available at https://doi.org/10.1038/s41598-025-95464-2.

Correspondence and requests for materials should be addressed to G.A. or W.P.